European Journal of Medicinal Chemistry 66 (2013) 296–304

Contents lists available at SciVerse ScienceDirect

European Journal of Medicinal Chemistry

journal homepage: http://www.elsevier.com/locate/ejmech

Original article

Quercitylcinnamates, a new series of antidiabetic bioconjugates possessing α-glucosidase inhibition and antioxidant

Eakkaphon Rattanangkool [a], Preecha Kittikhunnatham [a], Thanakorn Damsud [a,b], Sumrit Wacharasindhu [a], Preecha Phuwapraisirisan [a,*]

[a] Natural Products Research Unit, Department of Chemistry, Faculty of Science, Chulalongkorn University, Bangkok 10330, Thailand
[b] Program of Biotechnology, Faculty of Science, Chulalongkorn University, Bangkok 10330, Thailand

ARTICLE INFO

Article history:
Received 12 March 2013
Received in revised form
15 May 2013
Accepted 30 May 2013
Available online 10 June 2013

Keywords:
Diabetes mellitus
Glucosidase
Caffeic acid
Multifunctional drug
Quercitol

ABSTRACT

Antidiabetic agents possessing dual functions, α-glucosidase inhibition and antioxidant, have been accepted to be more useful than currently used antidiabetic drugs because they not only suppress hyperglycemia but also prevent risk of complications. Herein, we design antidiabetic bioconjugates comprising of (+)-*proto*-quercitol as a glucomimic and cinnamic analogs as antioxidant moieties. Fifteen quercitylcinnamates were synthesized by direct coupling through ester bond in the presence of DCC and DMAP. Particular quercityl esters **6a**, **7a** and **8a** selectively inhibited rat intestinal maltase and sucrose 4–6 times more potently than their parents **6**, **7** and **8**. Of synthesized bioconjugates, **6a** was the most potent inhibitor against maltase and sucrose with IC_{50} values of 5.31 and 43.65 μM, respectively. Of interest, its inhibitory potency toward maltase was 6 times greater than its parent, caffeic acid (**6**), while its radical scavenging (SC_{50} 0.11 mM) was comparable to that of commercial antioxidant BHA. Subsequent investigation on mechanism underlying inhibitory effect of **6a** indicated that it blocked maltase and sucrose functions by mixed inhibition through competitive and noncompetitive manners.

1. Introduction

Type 2 diabetes is characterized by chronic hyperglycemia and the development of microangiopathic complications such as retinopathy, nephropathy and neuropathy. Aggressive control of blood glucose level is preliminary and effective therapy for diabetic patients and reduces risk of complications [1]. Current evidences suggest that excess plasma glucose drives overproduction of superoxide radicals and other reactive oxygen species, which impair the cells via oxidative stress and account for the pathogenesis of all diabetic complications [2–4]. Therefore, antidiabetic drugs possessing antihyperglycemic effect and radical scavenging would be potential for diabetic therapy.

In the course of our research on new α-glucosidase inhibitors, we recently reported the synthesis and inhibitory effects of aminoquercitols [5], conduritol F [6] and inositol analogs from naturally available (+)-*proto*-quercitol (Fig. 1). Although (+)-*proto*-quercitol has five contiguous hydroxy groups on cyclohexane ring, exclusive formation of single bis-acetonide is critical to obtain the desired product without stereogenic congeners, in few steps. In fact, (+)-*proto*-quercitol itself does not show inhibitory activity against α-glucosidase possibly due to its water soluble property that enhances ready absorption by small intestine. However, structural modification of (+)-*proto*-quercitol by installing a series of alkyl and acyl motifs [7] or eliminating hydroxyl group [6] led to new generations of quercitol-based analogs with enhanced activity. With the success of this approach in hand, we expand our application by connecting quercitol core with other bioactive residues.

Inspired by chlorogenic acid (Fig. 2A), a well-recognized natural product having both antioxidant [8] and antidiabetic activities [9], we plan to introduce caffeic acid and other related cinnamic analogs onto quercitol core (Fig. 2B). In the current study, we synthesized fifteen quercitylcinnamates by coupling of (+)-*proto*-quercitol (**10**) and its epimer (**11**) (Scheme 1) with a series of cinnamic analogs (**1**–**8**, Scheme 2). A new series of quercitol-based bioconjugates with improved inhibition were obtained. Structure–activity relationship of the synthesized compounds and mechanism underlying α-glucosidase inhibitory effect of the most potent inhibitor are herein discussed.

* Corresponding author. Tel.: +66 2 2187624; fax: +66 2 2187598.
E-mail address: preecha.p@chula.ac.th (P. Phuwapraisirisan).

0223-5234/$ – see front matter © 2013 Elsevier Masson SAS. All rights reserved.
http://dx.doi.org/10.1016/j.ejmech.2013.05.047

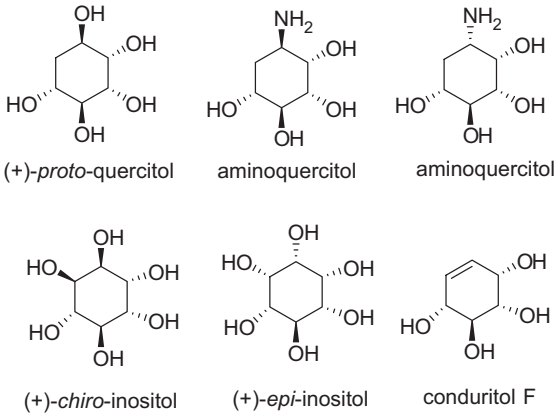

Fig. 1. Structures of (+)-*proto*-quercitol and its synthetic analogs.

2. Results and discussion

2.1. Compound design and synthesis

Crucial to the successful synthesis of all the conjugates described in this work is the selective coupling reaction of cinnamic derivatives with the desired hydroxy group on naturally available (+)-*proto*-quercitol (**9**) (Scheme 1). Bis-acetonides **10** and **11** were prepared from **9**, which was isolated from the stems of *Arfeuillea arborescens* using the procedure described elsewhere [6,7]. Briefly, (+)-*proto*-quercitol was obtained in 0.3% (w/w) yield as white solid after recrystallization by MeOH. Protection of two diols with dimethoxypropane gave the target alcohol **10**. In order to investigate the effect of C-1′ configuration on inhibitory effect, the epimer **11** was also synthesized from **10** through oxidation using acetic anhydride/DMSO followed by $LiAlH_4$ reduction, yielding the desired product in 42% yield.

With the chiral coupling partners **10** and **11** in hands, the quercitylcinnamates **1a**–**8b** were prepared as depicted in Scheme 2. For the esters **1a**–**8a** and their epimers **1b**–**8b**, the synthetic route was straight forward involving the direct coupling reaction between alcohol **10** or **11** with the corresponding cinnamic derivatives **1**–**5** in the presence of *N*,*N*′-dicyclohexylcarbodiimide (DCC) and 4-dimethylaminopyridine (DMAP). Removal of acetonide group underwent smoothly upon treatment of amberlyst-15 in methanol to give esters **1a**–**5a** in 56–73% yields (Scheme 2).

On the other hand, esterification of caffeic acid (**6**), ferulic acid (**7**) and isoferulic acid (**8**) required additional protection step because free phenolic group(s) of those compounds could interfere with the coupling reaction. The silylation of **6**–**8** with *tert*-butyldimethylsilyl chloride (TBDMSCl) not only prevented phenolic group(s) possibly being esterified but also improved solubility of the acids **6**–**8** in CH_2Cl_2, thus facilitating esterification reaction. The syntheses of quercitylcinnamates **6a**–**8b** were accomplished by ester bond formation of protected cinnamic derivatives with the chiral alcohol **10** or **11** followed by double deprotection of silyl and acetonide groups with TBAF and amberlyst-15, respectively. Esters **6a**–**8b** were then isolated in 42–49% yield as white solid (Scheme 2).

2.2. α-Glucose inhibitory activity and DPPH radical scavenging

All newly synthesized bioconjugates **1a**–**8b** were subjected to evaluate for their α-glucosidase inhibitory effect and antioxidation (Table 1). The commercial antidiabetic drug acarbose was used as the reference and the parent cinnamic analogs (**1**–**8**) were also validated for comparative purpose. For α-glucosidase inhibitory activity, all bioconjugates showed no inhibition against yeast α-glucosidase (type I α-glucosidase) but some of which inhibited maltase and sucrose, type II α-glucosidases from rat intestine. The bioconjugates **6a**–**8b**, whose structures encompassing caffeoyl, feruloyl and isoferulyl moieties, displayed inhibitory effects in range of 5.31–954.08 μM, whereas **1a**–**5a** were not active. Notably, their cinnamoyl cores in **6a**–**8b** different from those of **1a**–**5b** in having at least one phenolic group, suggesting that this moiety possibly involved in exerting the observed inhibition. It was likely that the more phenolic group in cinnamoyl moiety, the more potent inhibition observed. This result was similar to previous report of intestinal α-glucosidase inhibition of hydroxylated cinnamic derivatives **6**, **7** and **8** [10]. This trend was obviously found in **6a**, whose inhibition against maltase was more potent than those of **7a** (10 times) and **8a** (4 times); while **8a** showed only two times more potent than **7a** (Table 2).

Further inspection of two quercityl residues (**10** and **11**), installed in the active bioconjugates, on inhibitory effect revealed significant difference in inhibition. Bioconjugates **6a**, **7a** and **8a**, all of which generated from natural quercitol **10**, showed inhibitory effect 3–94 times more potent than their corresponding C-1′epimers (**6b**, **7b** and **8b**). The difference in inhibitory potency among epimeric analogs was strikingly observed in **6a**, whose inhibition against maltase and sucrose were 93 and 22 times more potent than **6b**. Compared to their corresponding cinnamic precursors (**6**, **7** and **8**), **6a**, **7a** and **8a** showed more improved inhibitory effects (4–6 times), whereas their epimeric analogs (**6b**, **7b** and **8b**) displayed reverse trend (Fig. 3). The observed results suggested that *R* configuration of C-1′ in quercityl moiety was also associated with exerting inhibitory effect, in addition to the presence of more phenolic groups in cinnamoyl residues. The pronounced inhibitions raised by *R* configuration of C-1′ were also supported by a similar trend observed in our previous report of *N*-alkyl aminoquercitols [7]. Of bioconjugates synthesized, **6a** showed most potent inhibition against both maltase and sucrase with IC_{50} values of 5.31 and 43.65 μM, respectively.

As for antioxidation of synthesized bioconjugates, **6a** showed radical scavenging activity toward DPPH with SC_{50} value of

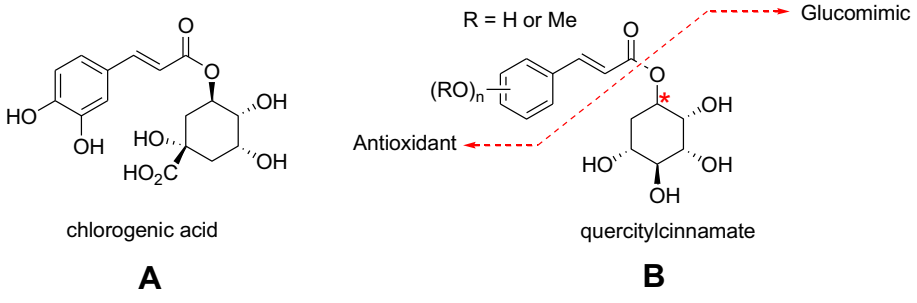

Fig. 2. Structures of chlorogenic acid (**A**) and designed quercitylcinnamates (**B**) encompassing antioxidant and glucomimic residues.

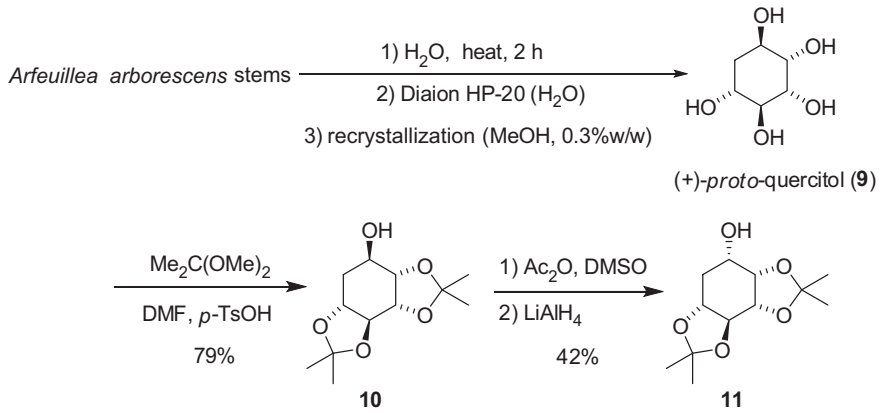

Scheme 1. Isolation of (+)-*proto*-quercitol and synthesis of bis-acetonides **10** and **11**.

0.11 mM, which was comparable to that of standard antioxidant BHA (SC_{50} 0.10 mM).

2.3. Mechanism underlying inhibitory effect of quercitylcaffeate against rat intestinal α-glucosidase

Since **6a** was the most potent inhibitor in hand, we therefore further study mechanism underlying this inhibitory effect. The Lineweaver–Burk plot of initial velocity versus maltose concentrations in the presence of different concentrations of **6a** gave a series of straight lines, all of which intersected within the second quadrant (Fig. 4). The analysis showed that V_{max} decreased with increasing K_m in the presence of increasing concentrations of **6a**. This behavior [11] indicated that **6a** inhibits maltase by two different pathways; competitively forming enzyme–inhibitor (EI) complex and interrupting enzyme–substrate (ES) intermediate by forming enzyme–substrate–inhibitor (ESI) complex in noncompetitive manner. To gain insightful the pathway in which **6a** preferentially proceeded, binding affinities of EI and ESI complexes were determined. Secondary plot of slope against concentration of **6a** (Fig. 5) showed EI dissociation constant (K_i) of 23.8 μM while ESI dissociation constant (K_i') of 64.5 μM was also deduced from secondary plot of intercept against concentration of **6a** (Fig. 6). A lower dissociation constant of K_i pointed out stronger binding between enzyme and **6a** and suggested preferred competitive over noncompetitive manners. In addition, inhibitory mechanism of **6a** toward sucrase was also determined using similar methodology. Apparently, **6a** also inhibited sucrase through mixed-inhibition (Fig. 7); in which competitive mode (K_i 22.4 μM, Fig. 8) was preferred over noncompetitive manner (K_i' 47.5 μM, Fig. 9).

3. Conclusions

In summary, we first synthesized fifteen bioconjugates (**1a**–**8b**) comprising two key moieties derived from (+)-*proto*-quercitol as glucomimic and cinnamic analogs as antioxidants. This synthetic design was implemented in the hope that the bioconjugates would provide dual activities, α-glucosidase inhibitory effect and antioxidant activity. Bioconjugates **6a**–**8b**, whose structures encompassing hydroxylated cinnamic analogs, displayed inhibition against rat maltase and sucrase in range of 5.31–954.08 μM. Notably, **6a** and **6b**, the bioconjugates having more phenolic groups in cinnamic core, were likely to provide pronounced inhibition. In addition, the *R* configuration of C-1′ in natural quercitol (**10**) also enhanced inhibitory effects over those of bioconjugates having unnatural quercitol (**11**). Therefore, coupling of quercityl and cinnamic moieties proved to enhance α-glucosidase inhibition. Prominent examples included **6a**, whose inhibitory effect against maltase was 6 times better than those of original caffeic acid (**6**). Of bioconjugates synthesized, **6a** was the most potent α-glucosidase inhibitor, in addition to its radical scavenging activity equipotent to standard antioxidant, BHA. In addition, mechanism underlying the inhibitory effect of **6a** against maltase and sucrase were proved to be mixed-type inhibition. This suggests proposed guideline for the application of **6a** as single antidiabetic agent or combination with other currently used drugs such as acarbose.

4. Experimental section

4.1. Chemistry

4.1.1. General procedure

All moisture-sensitive reactions were carried out under a nitrogen atmosphere. All solvents were distilled prior to use. HRESI-MS spectra were obtained from a micrOTOF Bruker mass spectrometer. ^1H and ^{13}C NMR spectra were recorded ($CDCl_3$ and CD_3OD as solvents) at 400 and 100 MHz, respectively, on a Varian Mercury$^+$ 400 NMR spectrometer. Chemical shifts were reported in ppm downfield from TMS or solvent residue. Thin layer chromatography (TLC) was performed on pre-coated Merck silica gel 60 F_{254} plates (0.25 mm thick layer) and visualized under 254 nm UV followed by dipping in $KMnO_4$ solution. Column chromatography was conducted using Merck silica gel 60 (70–230 mesh) or Sephadex LH-20.

4.1.2. Isolation of (+)-proto-quercitol (9) from the stems of A. arborescens

Our improved isolation of (+)-*proto*-quercitol (**9**) was applied [6,7]. Generally, ground stems (1.0–1.2 kg) of *A. arborescens* were boiled with water (2 × 4 L) for 2 h. The combined decoction was filtered, concentrated to a half and partitioned twice with equal volume of CH_2Cl_2 to remove lipophilic matters. The aqueous layer was diluted with water in a ratio of 2:1 and applied onto a Diaion HP20 column (1 kg) equilibrated with water. The column was excessively eluted with water (11 L), and the aqueous elutes were lyophilized to yield white powder. More purified (+)-*proto*-quercitol (**9**, 0.3% w/w) was obtained upon crystallization using hot MeOH.

4.1.3. Synthesis of bis-acetonides 10 and 11

Bis-acetonides were synthesized using our previous methods [5–7], yielding **10** (79%) and **11** (42%). The ^1H and ^{13}C NMR data were matched well the reports.

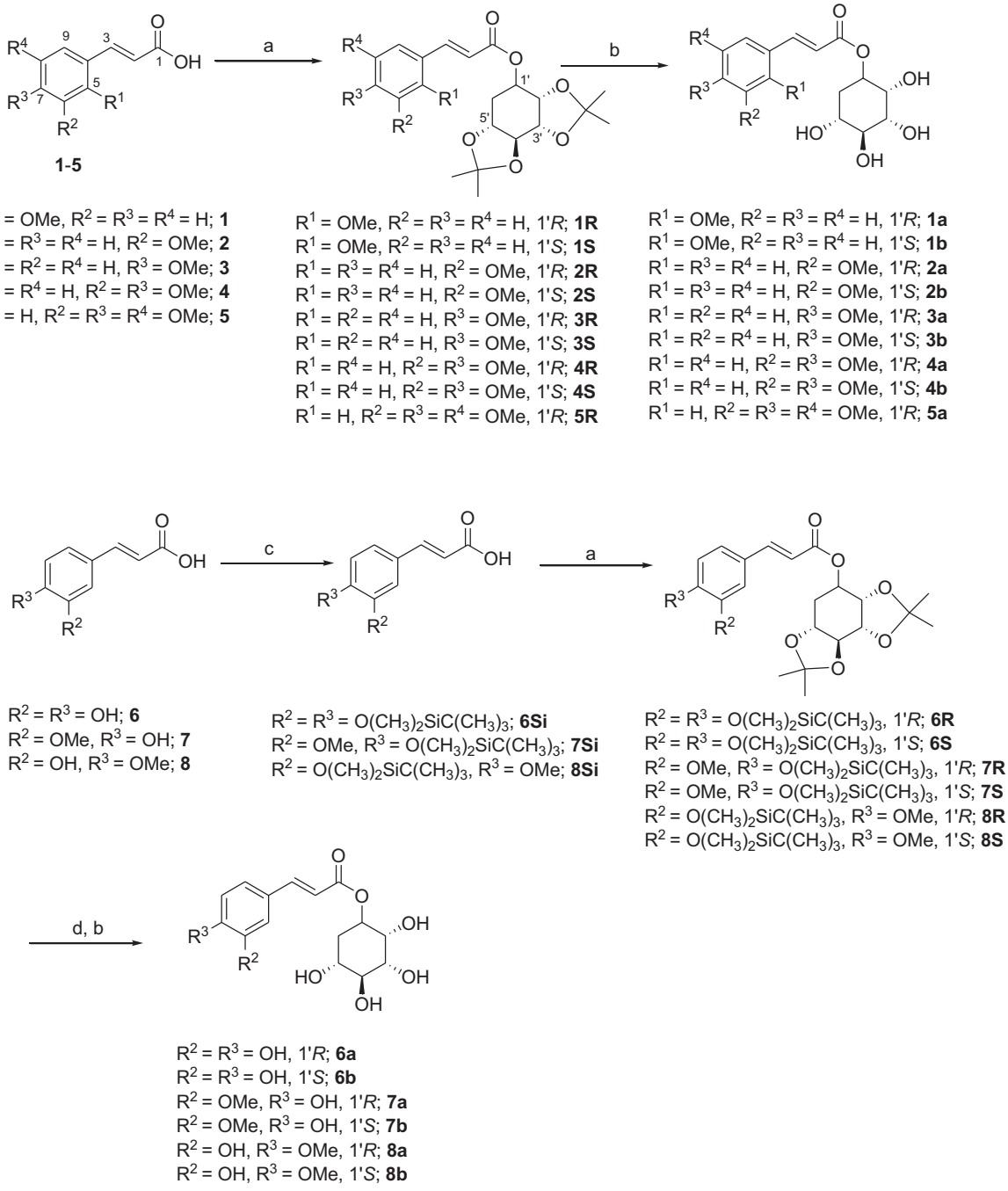

Scheme 2. Synthesis of quercitylcinnamates. Reagents and conditions: (a) **10** or **11**, DCC, DMAP, CH_2Cl_2, 0 °C to rt; (b) amberlyst-15, MeOH; (c) TBDMSCl, imidazole, DMF, rt; (d) TBAF, THF, rt.

4.1.4. General protection of phenolic groups

To a solution of **6**, **7** or **8** (1 eq, 2.57 mmol), imidazole (10 eq: 1 OH group) and *tert*-butyldimethylsilyl chloride (TBDMSCl) (10 eq: 1 OH group) in *N*,*N*-dimethylformamide (DMF, 15 mL) in a 50 mL round button flask. The mixture was stirred at room temperature for 1 h under N_2 gas. The reaction mixture was washed with water (3 × 20 mL) and the organic portion was extracted with ethyl acetate (EtOAc) (3 × 20 mL). The organic layer was washed with saturated aqueous NaCl, followed by dried over Na_2SO_4. After filtration and removal of the solvent under reduced pressure, the crude product was purified by silica gel column to afford **6Si**, **7Si** and **8Si** in 74, 82 and 79% yield, respectively.

*4.1.4.1. 3,4-Di-O-tert-butyldimetylsilylcaffeic acid (**6Si**).* White powder; ^{1}H NMR ($CDCl_3$, 400 MHz) δ 7.46 (d, J = 15.8 Hz, 1H), 6.83 (d, J = 8.8 Hz, 1H), 6.81 (s, 1H), 6.62 (d, J = 8.8 Hz, 1H), 6.03 (d, J = 15.8 Hz, 1H), 0.77 (d, J = 4.5 Hz, 18H), 0.00 (d, J = 3.2 Hz, 12H).

*4.1.4.2. 4-O-tert-Butyldimetylsilylferulic acid (**7Si**).* White powder; ^{1}H NMR ($CDCl_3$, 400 MHz) δ 7.65 (d, J = 15.9 Hz, 1H), 6.98 (d, J = 8.6 Hz, 1H), 6.95 (s, 1H), 6.79 (d, J = 8.6 Hz, 1H), 6.24 (d, J = 15.9 Hz, 1H), 3.78 (s, 3H), 0.93 (s, 9H), 0.11 (s, 6H).

*4.1.4.3. 4-O-tert-Butyldimetylsilylisoferulic acid (**8Si**).* White powder; ^{1}H NMR ($CDCl_3$, 400 MHz) δ 7.66 (d, J = 15.7 Hz, 1H), 6.97 (d,

Table 1
α-Glucosidase inhibitory effect and radical scavenging activity of quercityl-cinnamates.

Compounds	α-Glucosidase inhibitory effect (IC_{50}, μM)			Radical scavenging (SC_{50}, mM)
	Baker's yeast glucosidase	Maltase	Sucrase	
1a	NI[a]	NI	NI	NS[b]
1b	NI	NI	NI	NS
2a	NI	NI	NI	NS
2b	NI	NI	NI	NS
3a	NI	NI	NI	NS
3b	NI	NI	NI	NS
4a	NI	NI	NI	NS
4b	NI	NI	NI	NS
5a	NI	NI	NI	NS
6	NI	34.69 ± 0.74	87.45 ± 0.62	0.15
6a	NI	5.31 ± 0.10	43.65 ± 0.30	0.11
6b	NI	497.48 ± 0.50	954.08 ± 0.50	NS
7a	NI	51.93 ± 0.20	67.21 ± 0.20	NS
7b	NI	21.07 ± 0.15	171.43 ± 0.35	NS
8a	NI	20.81 ± 0.14	53.00 ± 0.32	NS
8b	NI	367.15 ± 0.42	805.48 ± 0.65	NS
Acarbose®	403.9 ± 0.40	1.50 ± 0.14	2.30 ± 0.02	ND[c]
BHA	ND	ND	ND	0.10

[a] No inhibition (inhibitory effect less than 30% at concentration of 10 mg/mL).
[b] No scavenging (inhibitory effect less than 50% at concentration of 10 mg/mL).
[c] Not determined.

J = 8.8 Hz, 1H), 6.95 (s, 1H), 6.79 (d, *J* = 8.8 Hz, 1H), 6.20 (d, *J* = 15.7 Hz, 1H), 3.78 (s, 3H), 0.93 (s, 9H), 0.11 (s, 6H).

4.1.5. General coupling reaction between bis-acetonides and cinnamic or silylated cinnamate derivatives

To a solution of **1**, **2**, **3**, **4** and **5** (2.5 eq) in CH_2Cl_2 (5 mL) were added *N*,*N*′-dicyclohexylcarbodiimide (DCC, 2.7 eq) and 4-dimethyl aminopyridine (DMAP, catalytic amount). The reaction mixture was stirred at 0 °C for 30 min. **10** or **11** (1 eq) in CH_2Cl_2 was added dropwise at room temperature under N_2 gas. The product was filtrated and solvent was removed under reduced pressure. The crude product was subsequently purified by silica gel column to afford bis-acetonides **1R**–**5R**.

To a solution of **6Si**, **7Si** and **8Si** (11 eq) in CH_2Cl_2 (10 mL) were added DCC (12 eq) and DMAP (catalytic amount). The reaction mixture was stirred at 0 °C for 30 min. **10** or **11** (1 eq) in CH_2Cl_2 was added dropwise at room temperature under N_2 gas. The bis-acetonides **6R**–**8S** were obtained after purification using silica gel column.

*4.1.5.1. **1**R.* 75% yield of pale yellow oil; ^{1}H NMR ($CDCl_3$, 400 MHz) δ 7.94 (d, *J* = 16.1 Hz, 1H), 7.43 (d, *J* = 7.6 Hz, 1H), 7.30 (t, *J* = 7.5 Hz,

Table 2
Kinetic data of α-glucosidase inhibition of **6a**.

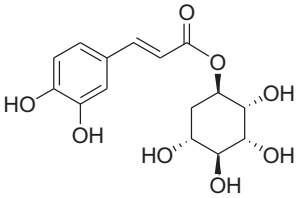

α-Glucosidase	Inhibition type	K_i (μM)	K_i' (μM)	K_m (mM)
Maltase	Mixed-inhibition	23.8	64.5	17.3
sucrase	Mixed-inhibition	22.4	47.5	25.9

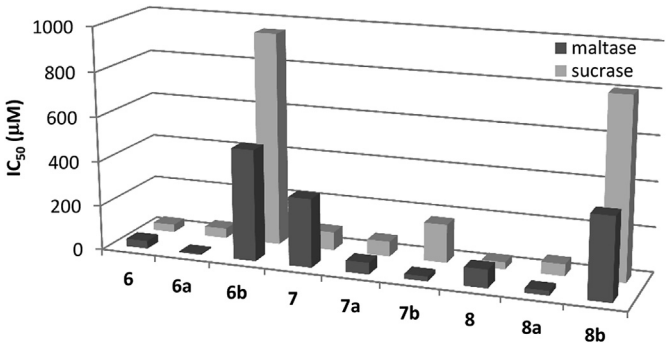

Fig. 3. Inhibition trends of bioconjugates **6a**–**8b** compared to their cinnamic parents **6**–**8**.

1H), 6.90 (t, *J* = 7.5 Hz, 1H), 6.85 (d, *J* = 7.6 Hz, 1H), 6.46 (d, *J* = 16.1 Hz, 1H), 5.47 (m, 1H), 4.30 (m, 1H), 4.23 (m, 1H), 3.83 (s, 3H), 3.66 (m, 1H), 3.54 (m, 1H), 2.16 (m, 1H), 2.04 (m, 1H), 1.46 (s, 3H), 1.38 (s, 6H), 1.30 (s, 3H).

*4.1.5.2. **1**S.* 72% yield of colorless wax; ^{1}H NMR ($CDCl_3$, 400 MHz) δ 7.98 (d, *J* = 16.1 Hz, 1H), 7.45 (d, *J* = 7.5 Hz, 1H), 7.29 (t, *J* = 7.6 Hz, 1H), 7.19 (s, 1H), 6.90 (t, *J* = 7.6 Hz, 1H), 6.85 (d, *J* = 7.5 Hz, 1H), 6.55 (d, *J* = 16.1 Hz, 1H), 5.30 (m, 1H), 4.37 (m, 1H), 4.23 (m, 1H), 3.84 (m, 4H), 3.44 (m, 1H), 2.36 (m, 1H), 1.93 (m, 2H), 1.47 (s, 3H), 1.40 (s, 3H), 1.38 (s, 3H), 1.30 (s, 3H).

*4.1.5.3. **2**R.* 79% yield of colorless wax; ^{1}H NMR ($CDCl_3$, 400 MHz) δ 7.61 (d, *J* = 16.0 Hz, 1H), 7.24 (t, *J* = 7.9 Hz, 1H), 7.06 (d, *J* = 7.5 Hz, 1H), 6.98 (s, 1H), 6.89 (d, *J* = 7.5 Hz, 1H), 6.36 (d, *J* = 16.0 Hz, 1H), 5.45 (m, 1H), 4.30 (m, 1H), 4.23 (m, 1H), 3.77 (s, 3H), 3.66 (m, 1H), 3.56 (m, 1H), 2.15 (m, 1H), 2.06 (m, 1H), 1.46 (s, 3H), 1.39 (s, 6H), 1.20 (s, 3H).

*4.1.5.4. **2**S.* 76% yield of colorless oil; ^{1}H NMR ($CDCl_3$, 400 MHz) δ 7.65 (d, *J* = 16.0 Hz, 1H), 7.24 (t, *J* = 7.9 Hz, 1H), 7.07 (d, *J* = 7.5 Hz, 1H), 6.99 (s, 1H), 6.89 (d, *J* = 7.5 Hz, 1H), 6.45 (d, *J* = 16.0 Hz, 1H), 5.31 (m, 1H), 4.38 (m, 1H), 4.24 (m, 1H), 3.83 (m, 1H), 3.77 (s, 3H), 3.45 (m, 1H), 2.38 (m, 1H), 1.92 (m, 1H), 1.47 (s, 3H), 1.40 (s, 3H), 1.38 (s, 3H), 1.30 (s, 3H).

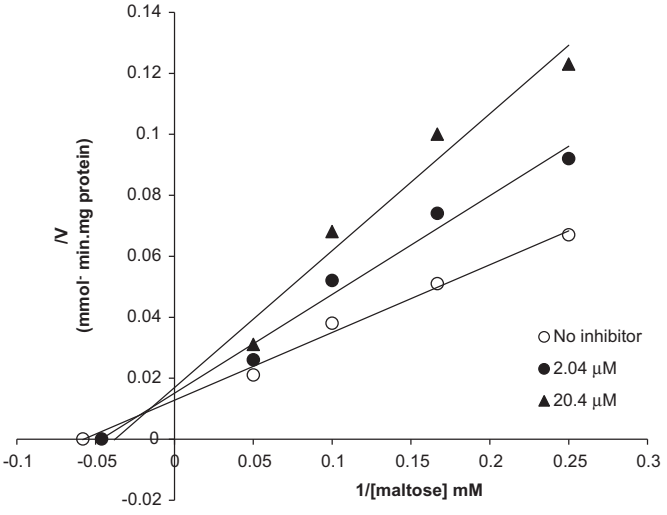

Fig. 4. Lineweaver–Burk plots for inhibitory activity of **6a** against maltase.

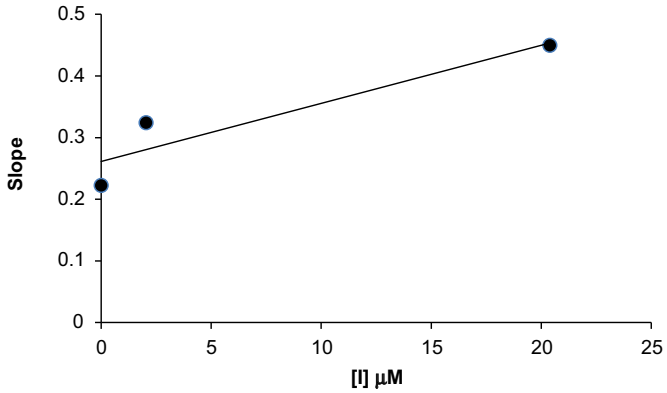

Fig. 5. Secondary plot of slope *vs* [*I*] for determination of K_i of **6a** against maltase.

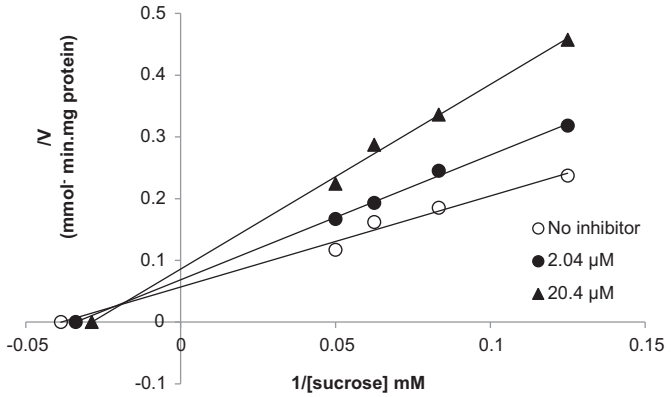

Fig. 7. Lineweaver–Burk plots for inhibitory activity of **6a** against sucrase.

4.1.5.5. ***3R***. 83% yield of colorless viscous oil; ^{1}H NMR ($CDCl_3$, 400 MHz) δ 7.60 (d, J = 16.0 Hz, 1H), 7.42 (d, J = 8.7 Hz, 2H), 7.19 (s, 4H), 6.84 (d, J = 8.7 Hz, 2H), 6.24 (d, J = 16.0 Hz, 1H), 5.45 (m, 1H), 4.30 (m, 1H), 4.23 (m, 1H), 3.78 (s, 3H), 3.65 (m, 1H), 3.54 (m, 1H), 2.15 (m, 1H), 2.05 (m, 1H), 1.47 (s, 3H), 1.39 (s, 6H), 1.31 (s, 3H).

4.1.5.6. ***3S***. 72% yield of colorless wax; ^{1}H NMR ($CDCl_3$, 400 MHz) δ 7.69 (d, J = 15.9 Hz, 1H), 7.49 (d, J = 8.4 Hz, 2H), 6.90 (d, J = 8.4 Hz, 2H), 6.38 (d, J = 15.9 Hz, 1H), 5.35 (m, 1H), 4.43 (m, 1H), 4.30 (m, 1H), 3.87 (m, 1H), 3.83 (s, 3H), 3.50 (m, 1H), 2.43 (m, 1H), 1.98 (m, 1H), 1.53 (s, 3H), 1.46 (s, 3H), 1.44 (s, 3H), 1.36 (s, 3H).

4.1.5.7. ***4R***. 78% yield of colorless oil; ^{1}H NMR ($CDCl_3$, 400 MHz) δ 7.64 (d, J = 15.9 Hz, 1H), 7.11 (d, J = 8.3 Hz, 1H), 7.05 (s, 1H), 6.87 (d, J = 8.3 Hz, 1H), 6.30 (d, J = 15.9 Hz, 1H), 5.52 (m, 1H), 4.36 (m, 1H), 4.30 (m, 1H), 3.92 (s, 9H), 3.72 (m, 1H), 3.61 (m, 1H), 2.21 (m, 1H), 2.12 (m, 1H), 1.53 (s, 3H), 1.45 (s, 6H), 1.37 (s, 3H).

4.1.5.8. ***4S***. 81% yield pale yellow oil; ^{1}H NMR ($CDCl_3$, 400 MHz) δ 7.62 (d, J = 15.8 Hz, 1H), 7.05 (d, J = 8.2 Hz, 1H), 7.01 (s, 1H), 6.81 (d, J = 8.2 Hz, 1H), 6.33 (d, J = 15.8 Hz, 1H), 5.31 (s, 1H), 4.38 (m, 1H), 4.24 (m, 1H), 3.83 (m, 7H), 3.45 (m, 2H), 2.37 (m, 1H), 1.90 (m, 1H), 1.48 (s, 3H), 1.40 (s, 3H), 1.38 (s, 3H), 1.30 (s, 3H).

4.1.5.9. ***5R***. 85% yield of colorless viscous oil; ^{1}H NMR ($CDCl_3$, 400 MHz) δ 7.56 (d, J = 15.9 Hz, 1H), 6.69 (s, 2H), 6.28 (d, J = 15.9 Hz, 1H), 5.45 (m, 1H), 4.31 (m, 1H), 4.24 (m, 1H), 3.82 (s, 9H), 3.66 (m, 1H), 3.54 (m, 1H), 2.21 (m, 1H), 2.12 (m, 1H), 1.47 (s, 3H), 1.39 (s, 6H), 1.31 (s, 3H).

4.1.5.10. ***6R***. 67% yield of colorless oil; ^{1}H NMR ($CDCl_3$, 400 MHz) δ 7.37 (d, J = 15.9 Hz, 1H), 6.80 (d, J = 8.7 Hz, 1H), 6.78 (s, 1H), 6.61 (d, J = 8.7 Hz, 1H), 6.00 (d, J = 15.9 Hz, 1H), 5.30 (m, 1H), 4.17 (m, 1H), 4.09 (m, 1H), 3.51 (m, 1H), 3.40 (m, 1H), 2.00 (m, 1H), 1.91 (m, 1H), 1.32 (s, 3H), 1.24 (s, 6H), 1.16 (s, 3H), 0.78 (s, 18H), 0.00 (s, 12H).

4.1.5.11. ***6S***. 77% yield of pale yellow oil; ^{1}H NMR ($CDCl_3$, 400 MHz) δ 7.56 (d, J = 15.9 Hz, 1H), 6.96 (d, J = 8.7 Hz, 1H), 6.94 (s, 1H), 6.75 (d, J = 8.7 Hz, 1H), 6.25 (d, J = 15.9 Hz, 1H), 5.29 (brs, 1H), 4.44 (m, 1H), 4.23 (m, 1H), 3.30 (m, 1H), 3.43 (m, 1H), 2.36 (m, 1H), 1.92 (s, 1H), 1.48 (s, 3H), 1.40 (s, 3H), 1.38 (s, 3H), 1.30 (s, 3H), 0.91 (s, 18H), 0.14 (s, 12H).

4.1.5.12. ***7R***. 68% yield of colorless oil ^{1}H NMR ($CDCl_3$, 400 MHz) δ 7.47 (d, J = 15.8 Hz, 1H), 6.86 (d, J = 7.2 Hz, 2H), 6.85 (s, 1H), 6.80 (d, J = 7.2 Hz, 1H), 6.12 (d, J = 15.8 Hz, 1H), 5.35 (m, 1H), 4.20 (m, 1H), 4.12 (m, 1H), 3.67 (s, 3H), 3.55 (m, 1H), 3.44 (m, 1H), 2.05 (m, 1H), 1.94 (m, 1H), 1.36 (s, 3H), 1.28 (s, 6H), 1.18 (m, 1H), 0.82 (s, 9H), 0.00 (s, 6H).

4.1.5.13. ***7S***. 69% yield of colorless oil; ^{1}H NMR ($CDCl_3$, 400 MHz) δ 7.50 (d, J = 15.9 Hz, 1H), 6.86 (d, J = 7.6 Hz, 1H), 6.83 (s, 1H), 6.67 (d, J = 7.6 Hz, 1H), 6.21 (d, J = 15.9 Hz, 1H), 5.20 (m, 1H), 4.27 (m, 1H), 4.13 (m, 1H), 3.72 (m, 1H), 3.67 (s, 3H), 3.34 (m, 1H), 2.27 (m, 1H), 1.81 (m, 1H), 1.37 (s, 3H), 1.30 (s, 3H), 1.27 (s, 3H), 1.20 (s, 3H), 0.82 (s, 9H), 0.00 (s, 6H).

4.1.5.14. ***8R***. 81% yield of pale yellow oil; ^{1}H NMR ($CDCl_3$, 400 MHz) δ 7.44 (d, J = 15.9 Hz, 1H), 6.94 (d, J = 8.2 Hz, 1H), 6.89 (s, 1H), 6.68

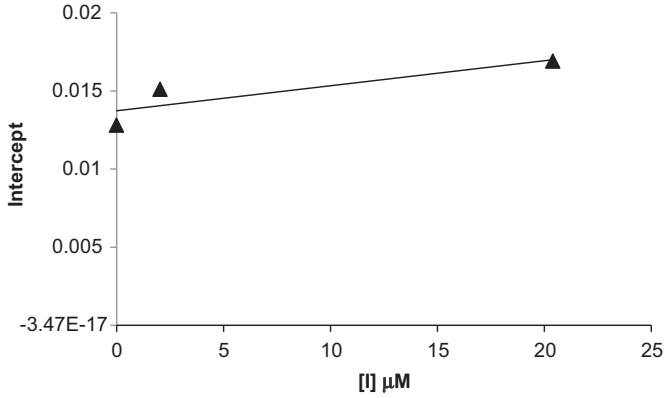

Fig. 6. Secondary plot of intercept *vs* [*I*] for determination of K_i' of **6a** against maltase.

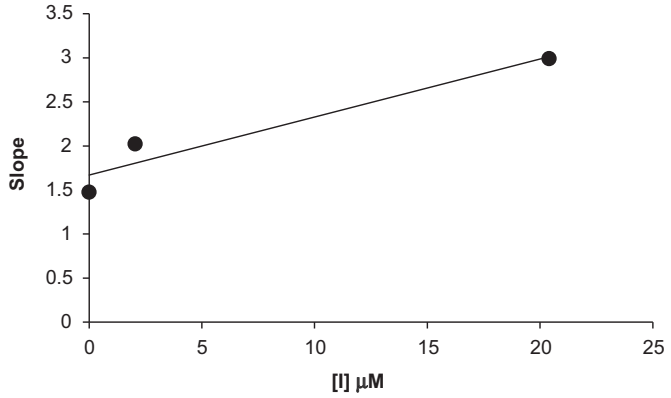

Fig. 8. Secondary plot of slope *vs* [*I*] for determination of K_i of **6a** against sucrase.

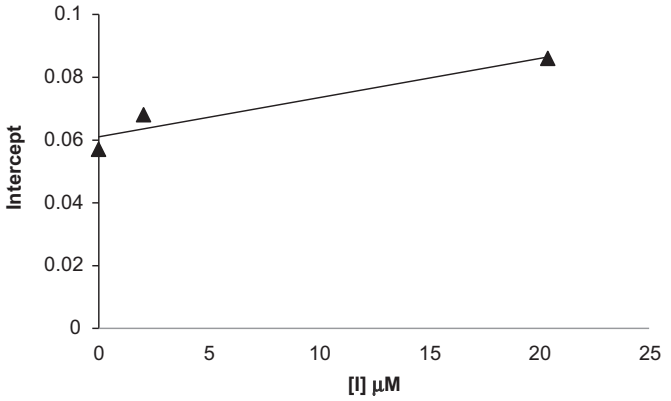

Fig. 9. Secondary plot of intercept *vs* [*I*] for determination of K_i' of **6a** against sucrase.

(d, *J* = 8.2 Hz, 1H), 6.08 (d, *J* = 15.9 Hz, 1H), 5.35 (m, 1H), 4.21 (m, 1H), 4.14 (m, 1H), 3.68 (s, 3H), 3.56 (m, 1H), 3.45 (m, 1H), 2.10–1.91 (m, 2H), 1.37 (s, 3H), 1.29 (s, 6H), 1.21 (s, 3H), 0.83 (s, 9H), 0.00 (s, 6H).

4.1.5.15. ***8S****.* 79% yield of colorless oil; ^{1}H NMR ($CDCl_3$, 400 MHz) δ 7.48 (d, *J* = 15.9 Hz, 1H), 6.95 (dd, *J* = 8.3, 2.0 Hz, 1H), 6.90 (d, *J* = 2.0 Hz, 1H), 6.68 (d, *J* = 8.3 Hz, 1H), 6.18 (d, *J* = 15.9 Hz, 1H), 5.20 (m, 1H), 4.28 (m, 1H), 4.13 (m, 1H), 3.72 (m, 1H), 3.68 (s, 3H), 3.34 (m, 1H), 2.27 (m, 1H), 1.83 (m, 1H), 1.38 (s, 3H), 1.30 (s, 3H), 1.28 (s, 3H), 1.21 (s, 3H), 0.84 (s, 9H), 0.00 (s, 6H).

4.1.6. General deprotection of silyl groups and bis-acetonides

Deprotection of **6R**–**8S**, which contained both silyl groups and bis-acetonides, was performed as follow. To a solution of **6R** (1 eq) in tetrahydrofuran (THF) was added TBAF/THF 1.0 M (2 eq: 1 OTBDMS). The mixture was stirred at room temperature for 3 h. The reaction mixture was washed with water (10 mL) and the organic layer was extracted with ethyl acetate (EtOAc) (3 × 15 mL) followed by being dried over Na_2SO_4. After filtration and removal of the solvent under reduced pressure, the crude product was dissolved in methanol (MeOH) and amberlyst-15 (0.5 g: 0.1 mmol) was added into the solution. The reaction mixture was stirred at room temperature for 5 h. After filtration and removal of the solvent under reduced pressure the crude product was purified by Sephadex LH-20 eluted with MeOH to afford **6a**. Compounds **6S**–**8S** were treated using aforementioned procedures to yield corresponding products **6b**–**8b**, respectively.

For deprotection of **1R**–**5R**, which contained only bis-acetonides, general procedures were conducted as follow. To a methanolic solution of **1R** was added amberlyst-15 (0.5 g: 0.1 mmol), and the reaction mixture was stirred at room temperature for 5 h. After filtration and removal of the solvent under reduced pressure, the crude product was purified by Sephadex LH-20 eluted with MeOH to afford **1a**. Compounds **1S**–**5R** were transformed, using the above procedures, to corresponding products **1b**–**5a**, respectively.

*4.1.6.1. 1′R-Quercityl-2-methoxycinnamate (****1a****).* 75% yield of colorless oil; ^{1}H NMR (CD_3OD, 400 MHz) δ 7.97 (d, *J* = 16.2 Hz, 1H, H-3), 7.56 (d, *J* = 6.8 Hz, 1H, Ar–H), 7.38 (t, *J* = 7.4 Hz, 1H, Ar–H), 7.03 (d, *J* = 6.8 Hz, 1H, Ar–H), 6.96 (t, *J* = 7.4 Hz, 1H, Ar–H), 6.53 (d, *J* = 16.2 Hz, 1H, H-2), 5.10 (m, 1H, H-1′), 3.94 (brs, 1H), 3.89 (s, 3H, OMe), 3.84–3.60 (m, 3H), 1.99 (m, 2H, H-6′); ^{13}C NMR (CD_3OD, 100 MHz) δ 168.0, 160.0, 142.1, 133.2, 130.0, 124.2, 121.9, 118.8, 112.5, 76.0, 73.5, 72.9, 71.5, 70.8, 56.2, 32.9; HRESIMS *m*/*z* 347.1100 $[M + Na]^+$ (calcd for $[C_{16}H_{16}$ Na $O_7]^+$ 347.1107).

*4.1.6.2. 1′S-Quercityl-2-methoxycinnamate (****1b****).* 79% yield of colorless oil; ^{1}H NMR (CD_3OD, 400 MHz) δ 7.92 (d, *J* = 16.2 Hz, 1H, H-3), 7.49 (dd, *J* = 8.0, 4.0 Hz, 1H, Ar–H), 7.28 (t, *J* = 7.5 Hz, 1H, Ar–H), 6.95 (d, *J* = 8.0 Hz, 1H, Ar–H), 6.88 (t, *J* = 7.5 Hz, 1H, Ar–H), 6.52 (d, *J* = 16.2 Hz, 1H, H-2), 4.85 (m, 1H, H-1′), 4.02 (s, 1H), 3.81 (s, 3H, OMe), 3.52–3.24 (m, 3H), 1.93 (m, 2H, H-6′); ^{13}C NMR (CD_3OD, 100 MHz) δ 168.6, 160.0, 142.0, 133.1, 130.0, 124.3, 121.9, 119.2, 112.5, 76.1, 73.6, 72.2, 71.5, 70.8, 56.1, 32.9; HRESIMS *m*/*z* 347.1108 $[M + Na]^+$ (calcd for $[C_{16}H_{20}NaO_7]^+$ 347.1107).

*4.1.6.3. 1′R-Quercityl-3-methoxycinnamate (****2a****).* 85% yield of colorless oil; ^{1}H NMR (CD_3OD, 400 MHz) δ 7.65 (d, *J* = 16.0 Hz, 1H, H-3), 7.32 (t, *J* = 7.8 Hz, 1H, Ar–H), 7.18 (d, *J* = 7.8 Hz, 1H, Ar–H), 7.15 (s, 1H, H-5), 6.98 (d, *J* = 7.8 Hz, 1H, Ar–H), 6.52 (d, *J* = 16.0 Hz, 1H, H-2), 5.11 (brs, 1H, H-1′), 3.93 (brs, 1H), 3.82 (s, 3H, OMe), 3.76–3.55 (m, 3H), 1.99 (m, 2H, H-6′); ^{13}C NMR (CD_3OD, 100 MHz) δ 167.4, 161.6, 146.7, 137.0, 131.1, 121.9, 118.9, 117.6, 114.1, 75.9, 73.4, 73.0, 71.5, 70.8, 55.9, 32.9; HRESIMS *m*/*z* 347.1110 $[M + Na]^+$ (calcd for $[C_{16}H_{16}NaO_7]^+$ 347.1107).

*4.1.6.4. 1′S-Quercityl-3-methoxycinnamate (****2b****).* 73% yield of colorless oil; ^{1}H NMR (CD_3OD, 400 MHz) δ 7.72 (d, *J* = 16.0 Hz, 1H, H-3), 7.31 (t, *J* = 7.8 Hz, 1H, Ar–H), 7.18 (d, *J* = 8.2 Hz, 1H, Ar–H), 7.15 (s, 1H, H-5), 6.97 (dd, *J* = 8.2, 1.6 Hz, 1H, H-9), 6.54 (d, *J* = 16.0 Hz, 1H, H-2), 4.85 (m, 1H, H-1′), 4.11 (s, 1H), 3.82 (s, 3H, OMe), 3.64–3.33 (m, 3H), 2.01 (m, 2H, H-6′); ^{13}C NMR (CD_3OD, 100 MHz) δ 167.8, 161.6, 146.6, 137.2, 131.1, 121.8, 119.2, 117.4, 114.1, 76.1, 73.6, 72.2, 71.6, 70.8, 55.8, 32.9; HRESIMS *m*/*z* 347.1107 $[M + Na]^+$ (calcd for $[C_{16}H_{20}NaO_7]^+$ 347.1107).

*4.1.6.5. 1′R-Quercityl-4-methoxycinnamate (****3a****).* 78% yield of white solid; ^{1}H NMR (CD_3OD, 400 MHz) δ 7.64 (d, *J* = 15.9 Hz, 1H, H-3), 7.56 (d, *J* = 8.6 Hz, 2H, H-5 and H-9), 6.95 (d, *J* = 8.6 Hz, 2H, H-6 and H-8), 6.37 (d, *J* = 15.9 Hz, 1H, H-2), 5.11 (m, 1H, H-1′), 3.96–3.59 (m, 4H), 3.83 (s, 3H, OMe), 1.99 (m, 2H, H-6′); ^{13}C NMR (CD_3OD, 100 MHz) δ 167.8, 163.3, 146.6, 131.1, 131.1, 128.2, 115.9, 115.5, 115.5, 76.0, 73.5, 72.8, 71.5, 70.8, 55.9, 33.0; HRESIMS *m*/*z* 347.1104 $[M + Na]^+$ (calcd for $[C_{16}H_{20}NaO_7]^+$ 347.1107).

*4.1.6.6. 1′S-Quercityl-4-methoxycinnamate (****3b****).* 78% yield of colorless oil; ^{1}H NMR (CD_3OD, 400 MHz) δ 7.61 (d, *J* = 15.9 Hz, 1H, H-3), 7.47 (d, *J* = 8.5 Hz, 2H, H-5 and H-9), 6.86 (d, *J* = 8.5 Hz, 2H, H-6 and H-8), 6.31 (d, *J* = 15.9 Hz, 1H, H-2), 4.85 (m, 1H, H-1′), 4.01 (s, 1H), 3.74 (s, 3H, OMe), 3.56–3.31 (m, 3H), 1.98–1.83 (m, 2H, H-6′); ^{13}C NMR (CD_3OD, 100 MHz) δ 168.3, 163.3, 146.5, 131.0, 131.0, 128.4, 116.2, 115.5, 115.5, 76.1, 73.6, 72.3, 71.4, 70.8, 55.9, 32.9; HRESIMS *m*/*z* 347.1103 $[M + Na]^+$ (calcd for $[C_{16}H_{20}NaO_7]^+$ 347.1107).

*4.1.6.7. 1′R-Quercityl-3,4-dimethoxycinnamate (****4a****).* 85% yield of colorless oil; ^{1}H NMR (CD_3OD, 400 MHz) δ 7.62 (d, *J* = 15.9 Hz, 1H, H-3), 7.22 (s, 1H, H-5), 7.17 (d, *J* = 8.2 Hz, 1H, Ar–H), 6.97 (d, *J* = 8.2 Hz, 1H, Ar–H), 6.40 (d, *J* = 15.9 Hz, 1H, H-2), 5.11 (m, 1H, H-1′), 3.97–3.56 (m, 4H), 3.86 (s, 6H, 2 × OMe), 2.00 (m, 2H, H-6′); ^{13}C NMR (CD_3OD, 100 MHz) δ 167.8, 153.0, 150.8, 146.9, 128.7, 124.2, 116.3, 112.7, 111.9, 76.0, 73.5, 72.9, 71.5, 70.8, 56.8, 56.5, 33.0; HRESIMS *m*/*z* 377.1203 $[M + Na]^+$ (calcd for $[C_{17}H_{22}NaO_8]^+$ 377.1212).

*4.1.6.8. 1′S-Quercityl-3,4-dimethoxycinnamate (****4b****).* 79% yield of colorless oil; ^{1}H NMR (CD_3OD, 400 MHz) δ 7.60 (d, *J* = 15.9 Hz, 1H, H-3), 7.12 (s, 1H, H-5), 7.09 (d, *J* = 8.2 Hz, 1H, Ar–H), 6.88 (d, *J* = 8.2 Hz, 1H, Ar–H), 6.33 (d, *J* = 15.9 Hz, 1H, H-2), 4.82 (m, 1H, H-1′), 4.01 (brs, 1H), 3.77 (s, 6H, 2 × OMe), 3.52–3.25 (m, 3H), 2.05–1.85 (m, 2H, H-6′); ^{13}C NMR (CD_3OD, 100 MHz) δ 168.2, 152.9, 150.8,

146.7, 128.9, 124.0, 116.5, 112.7, 111.6, 76.1, 73.6, 72.3, 71.4, 70.8, 56.5, 56.5, 33.0; HRESIMS *m/z* 377.1209 $[M + Na]^+$ (calcd for $[C_{17}H_{22}NaO_8]^+$ 377.1212).

*4.1.6.9. 1′R-Quercityl-3,4,5-trimethoxycinnamate (**5a**).* 83% yield of colorless oil; ^{1}H NMR (CD_3OD, 400 MHz) δ 7.62 (d, $J = 15.9$ Hz, 1H, H-3), 6.93 (s, 1H, Ar–H), 6.91 (s, 1H, Ar–H), 6.48 (d, $J = 15.9$ Hz, 1H, H-2), 5.12 (m, 1H, H-1′), 4.05–3.55 (m, 4H), 3.86 (s, 9H, 3 × OMe), 2.00 (m, 2H, H-6′); ^{13}C NMR (CD_3OD, 100 MHz) δ 167.5, 154.9, 146.8, 146.4, 131.5, 118.1, 118.0, 106.9, 106.8, 76.0, 73.5, 73.0, 71.5, 70.8, 61.2, 56.8, 56.8, 33.0; HRESIMS *m/z* 407.1310 $[M + Na]^+$ (calcd for $[C_{18}H_{24}NaO_9]^+$, 407.1318).

*4.1.6.10. 1′R-Quercitylcaffeate (**6a**).* 84% yield of yellow oil; ^{1}H NMR (CD_3OD, 400 MHz) δ 7.45 (d, $J = 15.9$ Hz, 1H, H-3), 6.95 (d, $J = 1.6$ Hz, 1H, H-5), 6.86 (dd, $J = 8.2$, 1.6 Hz, 1H, H-9), 6.69 (d, $J = 8.2$ Hz, 1H, H-8), 6.16 (d, $J = 15.9$ Hz, 1H, H-2), 5.00 (m, 1H, H-1′), 3.83 (brs, 1H), 3.68–3.45 (m, 3H), 1.89 (m, 2H, H-6′); ^{13}C NMR (CD_3OD, 100 MHz) δ 168.0, 149.7, 147.4, 146.9, 127.7, 123.1, 116.6, 115.3, 114.9, 76.0, 73.5, 72.8, 71.6, 70.8, 32.9; HRESIMS *m/z* 325.0930 $[M - H]^-$ (calcd for $[C_{15}H_{17}O_8]^-$ 325.0923).

*4.1.6.11. 1′S-Quercitylcaffeate (**6b**).* 84% yield of yellow oil; ^{1}H NMR (CD_3OD, 400 MHz) δ 7.51 (d, $J = 15.9$ Hz, 1H, H-3), 6.95 (d, $J = 1.8$ Hz, 1H, H-5), 6.88 (dd, $J = 8.1$, 1.8 Hz, 1H, H-9), 6.68 (d, $J = 8.1$ Hz, 1H, H-8), 6.20 (d, $J = 15.9$ Hz, 1H, H-2), 4.81 (m. 1H, H-1′), 4.00 (brs, 1H), 3.54–3.25 (m, 3H), 1.99–1.78 (m, 2H, H-6′); ^{13}C NMR (CD_3OD, 100 MHz) δ 168.5, 148.7, 147.3, 146.9, 127.8, 123.0, 116.5, 115.2, 115.2, 76.1, 73.6, 72.3, 71.3, 70.8, 32.9; HRESIMS *m/z* 349.0899 $[M + Na]^+$ (calcd for $[C_{15}H_{18}NaO_8]^+$ 349.0899).

*4.1.6.12. 1′R-Quercitylferurate (**7a**).* 79% yield of yellow less oil; ^{1}H NMR (CD_3OD, 400 MHz) δ 7.51 (d, $J = 15.9$ Hz, 1H, H-3), 7.11 (d, $J = 1.6$ Hz, 1H, H-5), 6.99 (dd, $J = 8.2$, 1.6 Hz, 1H, H-9), 6.72 (d, $J = 8.2$ Hz, 1H, H-8), 6.27 (d, $J = 15.9$ Hz, 1H, H-2), 5.01 (m, 1H, H-1′), 3.85–3.45 (m, 4H), 3.86 (s, 3H, OMe), 1.85 (m, 2H, H-6′); ^{13}C NMR (CD_3OD, 100 MHz) δ 168.0, 150.8, 149.4, 147.3, 127.6, 124.3, 116.5, 115.3, 111.8, 76.0, 73.4, 72.8, 71.5, 70.8, 56.5, 33.0; HRESIMS *m/z* 363.1057 $[M + Na]^+$ (calcd for $[C_{16}H_{20}NaO_8]^+$ 363.1056).

*4.1.6.13. 1′S-Quercitylferurate (**7b**).* 79% yield of colorless oil; ^{1}H NMR (CD_3OD, 400 MHz) δ 7.58 (d, $J = 15.9$ Hz, 1H, H-3), 7.09 (s, 1H, H-5), 6.99 (d, $J = 8.2$ Hz, 1H, Ar–H), 6.72 (d, $J = 8.2$ Hz, 1H, Ar–H), 6.29 (d, $J = 15.9$ Hz, 1H, H-2), 4.73 (m, 1H, H-1′), 4.01 (brs, 1H), 3.79 (s, 3H, OMe), 3.52–3.23 (m, 3H), 1.99–1.84 (m, 2H, H-6′); ^{13}C NMR (CD_3OD, 100 MHz) δ 168.5, 150.7, 149.4, 147.2, 127.8, 124.1, 116.6, 115.6, 111.9, 76.1, 73.6, 72.4, 71.3, 70.9, 56.5, 32.9; HRESIMS *m/z* 363.1057 $[M + Na]^+$ (calcd for $[C_{16}H_{20}NaO_8]^+$ 363.1056).

*4.1.6.14. 1′R-Quercitylisoferulate (**8a**).* 76% yield of yellow oil; ^{1}H NMR (CD_3OD, 400 MHz) δ 7.56 (d, $J = 15.9$ Hz, 1H, H-3), 7.08 (s, 1H, H-5), 7.07 (d, $J = 8.2$ Hz, 1H, Ar–H), 6.95 (d, $J = 8.2$ Hz, 1H, Ar–H), 6.30 (d, $J = 15.9$ Hz, 1H, H-2), 5.10 (m, 1H, H-1′), 3.92 (s, 1H), 3.89 (s, 3H, OMe), 3.77–3.58 (m, 3H), 1.99 (m, 2H, H-6′); ^{13}C NMR (CD_3OD, 100 MHz) δ 167.8, 151.7, 148.0, 147.0, 128.8, 123.0, 115.9, 114.8, 112.6, 76.0, 73.4, 72.8, 71.5, 70.8, 56.4, 32.9; HRESIMS *m/z* 363.1054 $[M + Na]^+$ (calcd for $[C_{16}H_{20}NaO_8]^+$ 363.1056).

*4.1.6.15. 1′S-Quercitylisoferulate (**8b**).* 64% yield of yellow oil; ^{1}H NMR (CD_3OD, 400 MHz) δ 7.54 (d, $J = 15.9$ Hz, 1H, H-3), 6.99 (s, 1H, H-5), 6.97 (d, $J = 8.2$ Hz, 1H, Ar–H), 6.85 (d, $J = 8.2$ Hz, 1H, Ar–H), 6.25 (d, $J = 15.9$ Hz, 1H, H-2), 4.73 (m, 1H, H-1′), 4.00 (brs, 1H), 3.79 (s, 3H, OMe), 3.48 (t, $J = 9.3$ Hz, 1H), 3.41–3.32 (m, 1H), 3.26 (m, 1H), 1.92 (m, 2H, H-6′); ^{13}C NMR (CD_3OD, 100 MHz) δ 168.3, 151.6, 148.1, 146.9, 129.0, 122.8, 116.2, 114.8, 112.6, 76.1, 73.6, 72.3, 71.4, 70.9, 56.5, 32.9; HRESIMS *m/z* 363.1056 $[M + Na]^+$ (calcd for $[C_{16}H_{20}NaO_8]^+$ 363.1056).

4.2. α-Glucosidase inhibitory activity

Inhibitory activity of test compound against α-glucosidase from baker's yeast was assessed based on *p*-nitrophenoxide colorimetric method [12]. Briefly, A 10 μL of test compound (1 mg/mL in DMSO) was pre-incubated with 40 μL of α-glucosidase (0.1 U/mL in 0.1 M phosphate buffer, pH 6.9) at 37 °C for 10 min. The mixture was added with 50 μL substrate solution (1 mM *p*-nitrophenyl-α-D-glucopyranoside, PNPG) and incubated for additional 20 min. The resulting mixture was quenched by adding 100 μL of 1 M Na_2CO_3. *p*-Nitrophenoxide ion liberated from the enzymatic reaction was monitored at 405 nm by Bio-Rad 3550 microplate reader. The percentage inhibition was calculated by $[(A_0 - A_1)/A_0] \times 100$, where A_1 and A_0 are the absorbance with and without the sample, respectively. The IC_{50} value was deduced from a plot of percentage inhibition versus sample concentration and acarbose was used as a positive control.

The inhibitory activity of the test compounds against α-glucosidases from rat intestine (as maltase and sucrase) was validated on the basis of glucose oxidase colorimetric method [13]. Maltase and sucrase was obtained from rat intestinal acetone powder (Sigma, St. Louis). Generally, the powder (1 g) was homogenized with 0.9% NaCl solution (30 mL). The aliquot containing both maltase and sucrase was obtained upon centrifugation (12,000 g) for 30 min. The test compound (1 mg/mL, 10 μL) was pre-incubated with crude enzyme solution (as maltase, 20 μL; as sucrase, 20 μL, respectively) at 37 °C for 10 min. The substrate solution (maltose: 0.58 mM, 20 μL; sucrose: 20 mM, 20 μL, respectively) in 0.1 M phosphate buffer (pH 6.9) was therefore added to the reaction mixture and incubated at 37 °C for additional 40 min. The mixture was heated in oven at 80 °C for 15 min to quench the reaction. The concentration of glucose released from the reaction mixture was determined by the glucose oxidase method using a commercial glucose assay kit (SU-GLLQ2, Human). The percentage inhibition was calculated using the above expression.

4.3. Kinetic study of α-glucosidase inhibition

The type of inhibition was investigated by analyzing enzyme kinetic data using aforementioned reactions. Maltase and sucrase activities were maintained at 0.45 and 0.09 U/mg protein, respectively, in the presence of inhibitor (from 0 to 20.4 μM) at various concentrations of maltose ranging from 1.0 to 20.0 mM. A series of V_{max} and K_m values were obtained from *Y* intercepts and calculated by slope × V_{max}, respectively.

4.4. DPPH radical scavenging

Radical scavenging activity was validated using DPPH colorimetric method [14]. Briefly, a sample solution (10 μL at concentrations of 0.1, 1.0 and 10.0 mg/mL) was added to 0.1 mM methanolic solution of DPPH (150 μL). The mixture was kept dark at room temperature in incubator shaker for 15 min. The absorbance of the resulting solution was measured at 517 nm with a 96-well microplate reader. The percentage scavenging was calculated by $[(A_0 - A_1)/A_0] \times 100$, where A_0 is the absorbance without the sample whereas A_1 is the absorbance with the sample. The SC_{50} value was deduced from a plot of percentage scavenging versus sample concentration. BHA was used as a standard antioxidant.

Acknowledgments

This work (DBG5380037) was supported by Thailand Research Fund and Chulalongkorn University. ER and TD are PhD candidates supported by Chulalongkorn University Dutsadi Phiphat Scholarship and The Commission of Higher Education, respectively. PK is an undergraduate student supported through the Development and Promotion of Science and Technology Talents Project (DPST).

Appendix A. Supplementary data

Supplementary data related to this article can be found at http://dx.doi:10.1016/j.ejmech.2013.05.047.

References

[1] P. Zimmet, K.G.M.M. Alberti, J. Shaw, Global and societal implications of the diabetes epidemic, Nature 414 (2001) 782–787.
[2] V. Bocci, I. Zanardi, M.S.P. Huijberts, V. Travagli, Diabetes and chronic oxidative stress. A perspective based on the possible usefulness of ozone therapy, Diabetes Metab. Syndr. Clin. Res. Rev. 2 (2011) 45–49.
[3] M. Brownlee, Biochemistry and molecular cell biology of diabetic complications, Nature 414 (2001) 813–820.
[4] A.C. Maritim, R.A. Sanders, J.B. Watkins III, Diabetes, oxidative stress, and antioxidants: a review, J. Biochem. Mol. Toxicol. 17 (2003) 24–38.
[5] S. Wacharasindhu, W. Worawalai, W. Rungprom, P. Phuwapraisirisan, (+)-*proto*-Quercitol, a natural versatile chiral building block for the synthesis of the alpha-glucosidase inhibitors, 5-amino-1,2,3,4-cyclohexanetetrols, Tetrahedron Lett. 50 (2009) 2189–2192.
[6] W. Worawalai, E. Rattanangkool, A. Vanitcha, P. Phuwapraisirisan, S. Wacharasindhu, Concise synthesis of (+)-conduritol F and inositol analogues from naturally available (+)-*proto*-quercitol and their glucosidase inhibitory activity, Bioorg. Med. Chem. Lett. 22 (2012) 1538–1540.
[7] W. Worawalai, S. Wacharasindhu, P. Phuwapraisirisan, Synthesis of new *N*-substituted aminoquercitols from naturally available (+)-*proto*-quercitol and their alpha-glucosidase inhibitory activity, Med. Chem. Commun. 3 (2012) 1466–1470.
[8] Y. Sato, S. Itagaki, T. Kurokawa, J. Ogura, M. Kobayashi, T. Hirano, M. Sugawara, K. Iseki, In vitro and in vivo antioxidant properties of chlorogenic acid and caffeic acid, Int. J. Pharm. 403 (2011) 136–138.
[9] A. Hunyadi, A. Martins, T.J. Hsieh, A. Seres, I. Zupkó, Chlorogenic acid and rutin play a major role in the in vivo anti-diabetic activity of *Morus alba* leaf extract on type II diabetic rats, PLoS One 11 (2012) e50619.
[10] S. Adisakwattana, P. Chantarasinlapin, H. Thammarat, S. Yibchok-Anun, A series of cinnamic acid derivatives and their inhibitory activity on intestinal alpha-glucosidase, J. Enzym. Inhib. Med. Chem. 24 (2009) 1194–1200.
[11] R.L. Stein, Kinetics of Enzyme Action: Essential Principles for Drug Hunters, John Wiley & Sons, Singapore, 2011.
[12] A. Schäfer, P. Högger, Pharmaceutical and nutraceutical effects of *Pinuspinaster* bark extract, Diabetes Res. Clin. Pract. 77 (2007) 41–46.
[13] D. Barham, P. Trinder, An improved colour reagent for the determination of blood glucose by the oxidase system, Analyst 97 (1972) 142–145.
[14] A.L. Dawidowicz, D. Wianowska, M. Olszowy, On practical problems in estimation of antioxidant activity of compounds by DPPH method (Problems in estimation of antioxidant activity), Food Chem. 131 (2012) 1037–1043.